VOLUME 113 NUMBER 24
NOVEMBER 20, 1991

JOURNAL
OF THE
AMERICAN
CHEMICAL
SOCIETY

The Nature of Intramolecular Hydrogen-Bonded and Non-Hydrogen-Bonded Conformations of Simple Di- and Triamides

Juan J. Novoa*,† and Myung-Hwan Whangbo*

Contribution from the Department of Chemistry, North Carolina State University, Raleigh, North Carolina 27695-8204. *Received May 20, 1991*

Abstract: The nature and the magnitude of the N—H···O=C hydrogen-bonding interaction in amides were examined in terms of ab initio and AM1 calculations on formamide dimer. On the basis of AM1 calculations, we examined the relative stabilities of various intramolecular hydrogen-bonded and non-hydrogen-bonded conformations for several di- and triamides. AM1 calculations were also performed for certain amide structures solvated with CH_2Cl_2 molecules. The energy surface of the N—H···O=C hydrogen-bonding interaction is soft with respect to the ∠N—H···O and the ∠H···O=C angle variation. For each of the amides studied, the most stable conformation is a hydrogen-bonded structure. For an amide which forms a hydrogen-bonded 6- or 7-membered ring containing one CH_2 group, the corresponding non-hydrogen-bonded form is not a stationary (i.e., minimum energy) structure but is made stationary when solvated with CH_2Cl_2 molecules. The stability of triamide **1** increases with an increase in the number of intramolecular hydrogen-bonding contacts. The conformation **1c** of this triamide, which makes 7- and 9-membered hydrogen-bonded rings involving the H_b atom but leaves the H_a atom non-hydrogen-bonded, is not a stationary structure even when solvated with CH_2Cl_2 molecules.

Proteins are inherently flexible molecules so that their folding patterns result from a delicate energetic balance of the interactions associated with many noncovalent contacts (e.g., intramolecular N—H···O=C hydrogen-bonding contacts).[1,2] Polyamides are not an ideal model for proteins since they lack the amino acid side chains. However, in both polyamides and proteins, the intramolecular N—H···O=C hydrogen-bonding interactions play an important role in determining their folding patterns. Thus, knowledge about the nature and the magnitudes of the intramolecular N—H···O=C hydrogen-bonding interactions in simple amides can be useful in understanding the folding patterns of polyamides as well as proteins. As an important first step toward elucidating the structural factors stabilizing folded protein conformations, Gellman and co-workers have recently carried out a series of variable-temperature NMR studies on simple amides **1–3**

Table I. Optimum H···O Distance (r_{opt}), Total Energy (E), and Interaction Energy (ΔE and ΔE_{cp}) Calculated for **5**

basis set	method	r_{opt}, Å	E, au	ΔE, kcal/mol	ΔE_{cp}, kcal/mol
6-31G**	SCF-MO	2.086	−337.890 405	−6.00	−5.38
	MP2	2.086[a]	−338.848 114	−6.47	−5.12
6-31++G**	SCF-MO	2.121	−337.906 290	−5.83	−5.56
	MP2	2.041	−338.878 752	−6.29	−5.40

[a] The r_{opt} value obtained at the SCF-MO level.

† On sabbatical leave from Departamento de Quimica Fisica, Facultad de Quimica. Universidad de Barcelona, 08028 Barcelona, Spain.

0002-7863/91/1513-9017$02.50/0

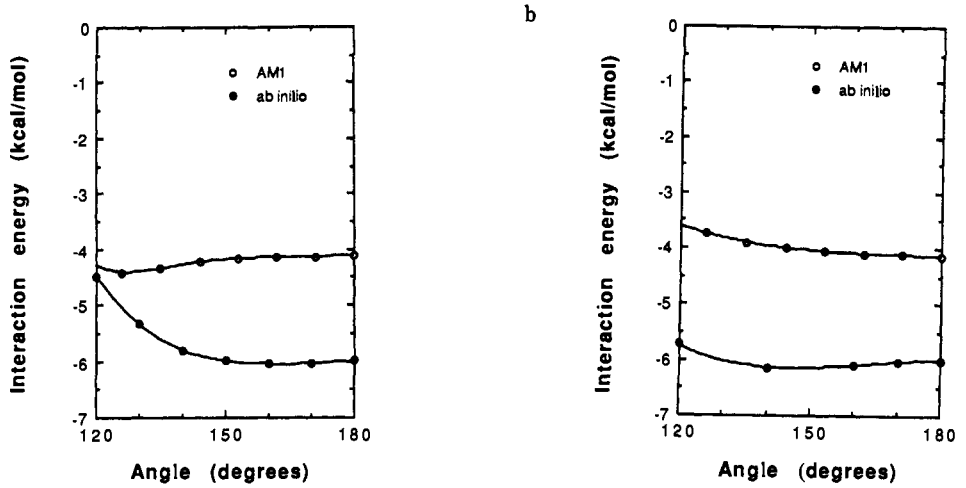

Figure 1. Comparison of the interaction energies ΔE of **5** obtained from ab initio and AM1 calculations: (a) ΔE values of **5** for linear H···O=C calculated as a function of ∠N—H···O and (b) ΔE values of **5** for linear N—H···O calculated as a function of ∠H···O=C.

Table II. Heats of Formation (ΔH_f), Relative Energies ($\Delta\Delta E$), H···O Contact Distances ($r_{H\cdots O}$), N—H···O Contact Angle (∠N—H···O), and H···O=C Contact Angle (∠H···O=C) Calculated for Several Structures of Diamides **2**(n = 1–4) and **3**

amide	structure	H-bonded ring size	$r_{H\cdots O}$, Å	∠N—H···O, deg	∠H···O=C, deg	ΔH_f, kcal/mol	$\Delta\Delta E$, kcal/mol
2(n = 1)	**2a**(n=1)	6	2.473	123.3	85.2	−77.87	0.00
	2b(n=1)	6	2.181	120.7	101.2	−77.23	0.64
	2c(n=1)[a,b]					−73.50	4.37
2(n = 2)	**2a**(n=2)	7	2.183	135.5	106.7	−85.07	0.00
	2b(n=2)	7	2.178	134.7	110.3	−84.95	0.12
	2c(n=2)[a]					−83.62	2.45
2(n = 3)	**2a**(n=3)	8	2.176	148.3	116.1	−91.17	0.00
	2b(n=3)	8	2.232	150.7	135.0	−90.97	0.20
	2c(n=3)[a]					−89.63	1.54
2(n = 4)	**2a**(n=4)	9	2.148	166.3	132.2	−97.65	0.00
	2b(n=4)	9	2.236	135.6	120.0	−96.63	1.02
	2c(n=4)	9	2.246	136.5	102.7	−95.62	2.03
	2d(n=4)	9	2.364	126.4	108.9	−95.30	2.35
	2e(n=4)[a]					−96.58	1.02
	2f(n=4)[a]					−95.02	2.63
3	**3a**	7	2.182	138.6	102.6	−88.26	0.00
	3b	7	2.190	138.8	103.3	−88.11	0.15
	3c[a,b]					−81.86	6.40

[a] Non-hydrogen-bonded structure. [b] Lowest energy transition state.

Table III. Heats of Formation (ΔH_f), Relative Energies ($\Delta\Delta E$), H···O Contact Distances ($r_{H\cdots O}$), N—H···O Contact Angle (∠N—H···O), and H···O=C Contact Angle (∠H···O=C) Calculated for Several Conformations of Triaminde **1**

amide	structure label	H-bonded ring size	$r_{H\cdots O}$, Å	∠N—H···O, deg	∠H···O=C, deg	ΔH_f, kcal/mol	$\Delta\Delta E$, kcal/mol
1	**1b**(d,u)	6	2.436	121.2	86.7	−115.80	0.00
		7	2.192	140.3	100.6		
	1b(d,d)	6	2.299	126.2	91.2	−115.79	0.01
		7	2.183	140.0	101.5		
	1b(u,u)	6	2.161	121.6	102.3	−115.45	0.35
		7	2.186	140.3	100.0		
	1b(u,d)	6	2.181	118.6	101.8	−115.11	0.69
		7	2.181	140.6	102.9		
	1e	6	2.331	110.5	94.8	−115.03	0.77
		9	2.215	161.6	135.4		

in dilute CD_2Cl_2 solution.[3-5] Their analysis of the temperature-dependent NMR data for triamide **1** in terms of an equilibrium involving three conformations **1a**, **1b**, and **1c** led to the conclusion that **1c** is enthalpically more stable than **1a** and **1b**.[4] This conclusion is consistent with the observation[6] that the crystal structure of **1** adopts the conformation **1c**, but is quite striking because both amide protons H_a and H_b participate in hydrogen bonding in **1b** while only one does in **1a** and **1c** so that one would have anticipated **1b** to be more stable than **1a** and **1c**. Thus a detailed knowledge about the folding characteristics of simple di- and triamides could lead to a vital insight into the complex folding patterns of polypeptides. In order to provide theoretical results necessary for understanding the folding characteristics of simple amides, we study in the present work the nature and the energetics of intramolecular hydrogen-bonded and non-hydrogen-bonded

(1) (a) Fasman, G. D. *Prediction of Protein Structure and the Principles of Protein Conformation*; Fasman, G. D., Ed.; Plenum Press: New York, 1989; pp 193–316. (b) Alber, T. *Ibid*, pp 161–192.
(2) Baker, E. N.; Hubbard, R. E. *Prog. Biophys. Mol. Biol.* **1984**, *44*, 97.
(3) Gellman, S. H.; Adams, B. R. *Tetrahedron Lett.* **1989**, *30*, 3381.
(4) Gellman, S. H.; Adams, B. R.; Dado, G. P. *J. Am. Chem. Soc.* **1990**, *112*, 460.
(5) Gellman, S. H.; Dado, G. P.; Liang, G.-B.; Adams, B. R. *J. Am. Chem. Soc.* **1991**, *113*, 1164.
(6) Dado, G. P.; Desper, J. M.; Gellman, S. H. *J. Am. Chem. Soc.* **1990**, *112*, 8630.

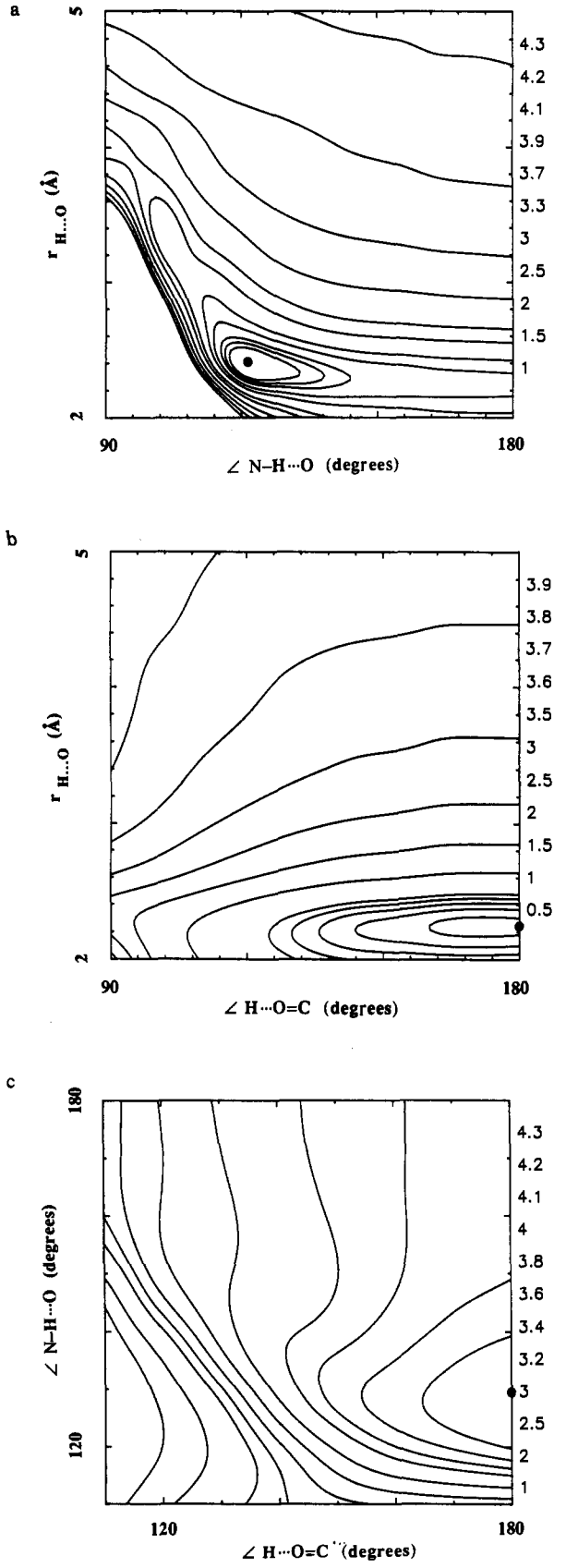

Figure 2. Contour plots of the interaction energies ΔE of **5** obtained from AM1 calculations: (a) ΔE values of **5** (for linear H···O═C) calculated as a function of $r_{H\cdots O}$ and ∠N—H···O; (b) ΔE values of **5** (for linear N—H···O) calculated as a function of $r_{H\cdots O}$ and ∠H···O═C, and (c) ΔE values of **5** calculated as a function of ∠N—H···O and ∠H···O═C. The minimum energy point in each plot is represented by a filled circle, and the negative values of the energy contours plotted (kcal/mol) are shown in the right-hand-side margins of the diagrams.

Chart I

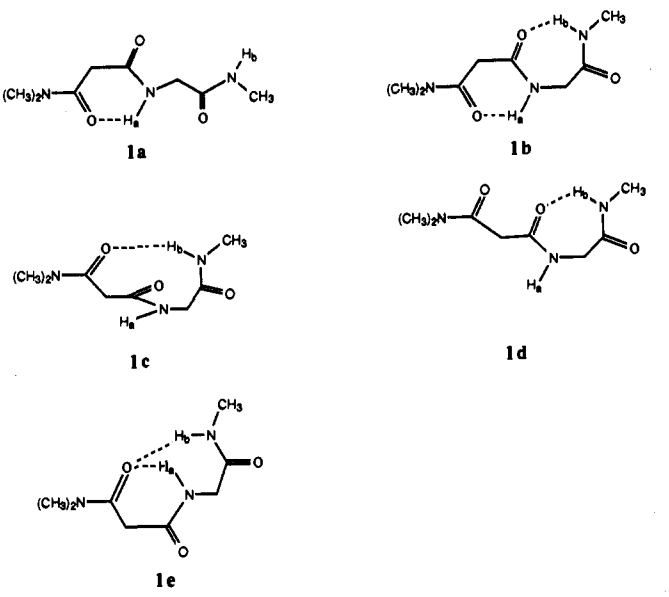

Chart II

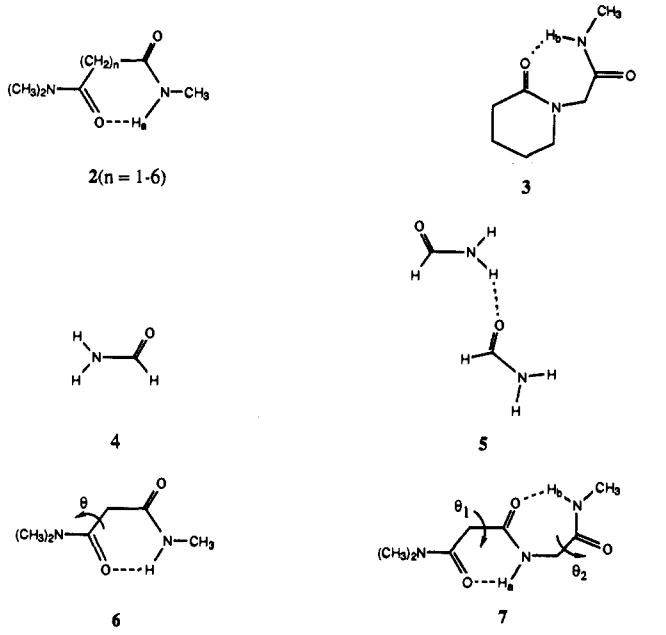

structures for amides **1–3** on the basis of AM1 semiempirical SCF-MO calculations. Since the available structural information about these amides was obtained from IR and NMR studies in CH_2Cl_2 and CD_2Cl_2 solvent,[3-5] we also calculate the energetics of amide structures solvated with CH_2Cl_2 molecules.

Computational Details

All our calculations require full geometry optimizations and are computationally demanding. Thus we employ the AM1 semiempirical SCF-MO method[7] because it provides an adequate description of hydrogen bonding and is computationally affordable. In order to establish that our AM1 calculations lead to qualitatively correct results concerning the relative stabilities of the hydrogen-bonded and non-hydrogen-bonded conformations of amides **1–3**, it is necessary to evaluate how well AM1 calculations describe the intramolecular N—H···O═C hydrogen bonding in **1–3**. Thus we performed ab initio SCF-MO and MP2[8] calculations

(7) (a) Dewar, M. J. S.; Zoebisch, E. G.; Healy, E. F.; Stewart, J. J. P. *J. Am. Chem. Soc.* **1985**, *107*, 3902. (b) Vinson, L. K.; Dannenberg, J. J. *J. Am. Chem. Soc.* **1989**, *111*, 2777 and references therein. (c) Reynolds, C. H. *J. Am. Chem. Soc.* **1990**, *112*, 7903.

(8) Moller, C.; Plesset, M. S. *Phys. Rev.* **1934**, *46*, 618.

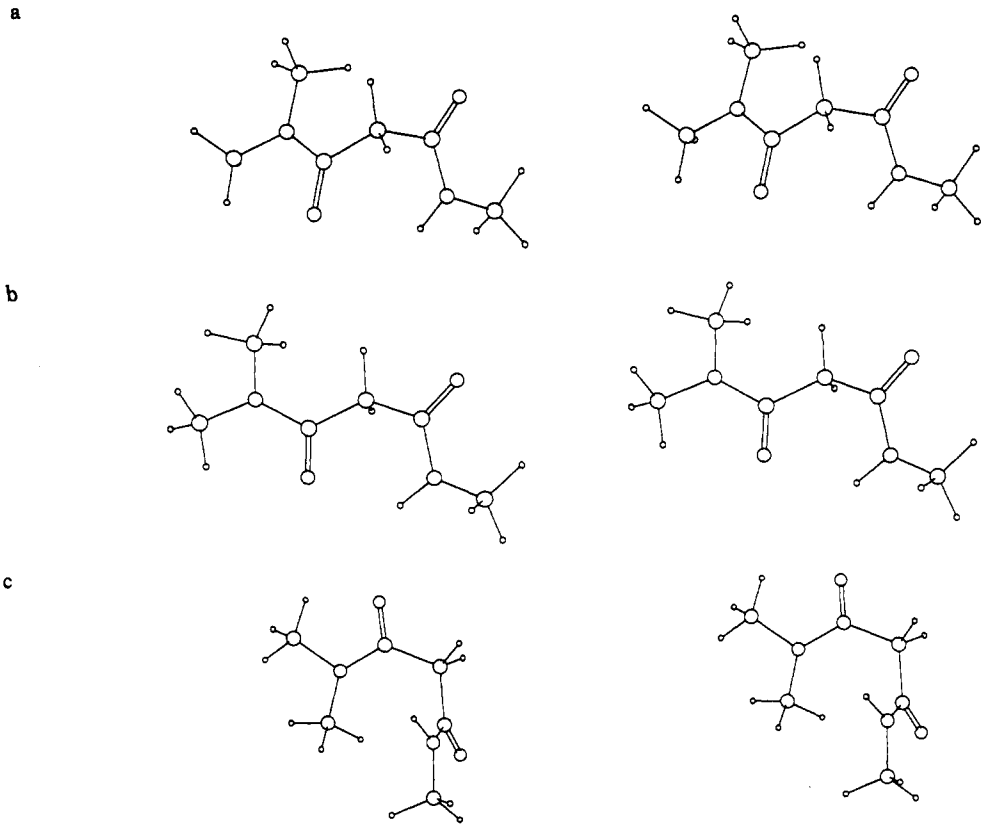

Figure 3. Stereoviews of several structures of diamide **2**(n=1): (a) **2a**(n=1), (b) **2b**(n=1), and (c) **2c**(n=1).

Table IV. Interaction Energies and Intermolecular Contact Distances Calculated for Several Arrangements of **8** and **9**

arrangement	intermolecular contact distance, Å	interaction energy, kcal/mol
8a	$r_{H\cdots O}$ = 2.402	−2.51
8b	$r_{H\cdots Cl}$ = 2.929	−0.17
8c	$r_{H\cdots O}$ = 2.179 $r_{H\cdots Cl}$ = 2.643	−3.27
9a	$r_{H\cdots Cl}$ = 2.900	−0.72
9b	$r_{H\cdots Cl}$ = 2.816	−0.75

on formamide **4** and formamide dimer **5** and compared the results of these calculations with those derived from the corresponding AM1 calculations. All our AM1 semiempirical SCF-MO calculations on amides **1–3** were carried out by employing the MOPAC program[9] installed in Tektronix CAChe Worksystem. Full geometry optimizations were done with the PRECISE option unless stated otherwise, and we did not employ the MMOK option. The present ab initio SCF-MO and MP2 calculations were performed by using the GAUSSIAN-86 program.[10]

Nature of N—H···O=C Hydrogen Bonding

Both AM1 calculations and ab initio SCF-MO calculations with the 6-31G** basis set[12] reveal that **4** is planar, and the rotational barrier of **4** around the C–N bond is calculated to be 10.1[7a] and 16.1 kcal/mol by the AM1 and ab initio calculations, respectively. The rotational barrier is estimated to be about 20 kcal/mol experimentally,[11] and is therefore somewhat underestimated by the AM1 calculation. Table I summarizes the optimum H···O contact distance (r_{opt}) and the interaction energy (ΔE) of **5** (for linear N—H···O and linear H···O= C) calculated by employing the

Chart III

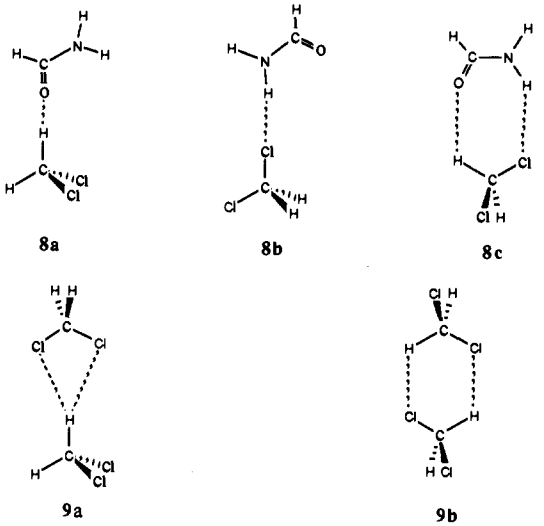

6-31G** and 6-31++G** basis sets[10] at the SCF-MO and MP2 levels. The ΔE_{cp} values of Table I are the interaction energies with the basis set superposition errors corrected by the counterpoise method.[12] In these SCF-MO and MP2 calculations, the formamide fragment geometries were kept frozen. (At the AM1 level, we checked the effect of relaxing the monomer geometries in the interaction energies. Since this effect is negligible, we present only those results obtained with the frozen monomer geometries.) The interaction energy of **5** is only slightly affected by the addition of diffuse functions in the basis set and by the inclusion of correlation energies. Thus SCF-MO calculations with the 6-31G** basis set are expected to be sufficient in assessing how sensitively the interaction energy of **5** depends upon the ∠N—H···O and the ∠H···O=C angles.

We calculate the ΔE values of **5** (for linear H···O=C) as a function of ∠N—H···O, and also those of **5** (for linear N—H···O)

(9) Stewart, J. J. P. *QCPE* No. 455.
(10) GAUSSIAN-86: Frisch, M. J.; Binkley, J. S.; Schlegel, H. B.; Ragavachari, K.; Melius, C. F.; Martin, R. L.; Stewart, J. J. P.; Bobrowicz, F. W.; Rohfling, C. M.; Kahn, L. R.; Defrees, D. J.; Seeger, R.; Whiteside, R. A.; Fox, D. J.; Fleuder, E. M.; Pople, J. A.; Carnegie-Mellon, Quantum Chemistry Publishing Unit: Pittsburgh, 1984.
(11) (a) Drakenberg, T.; Forsen, S. *J. Phys. Chem.* **1970**, *74*, 1. (b) Perricaudet, M.; Pullman, A. *Int. J. Peptide Protein Res.* **1973**, *5*, 99.
(12) Boys, S. F.; Bernardi, F. *Mol. Phys.* **1970**, *19*, 553.

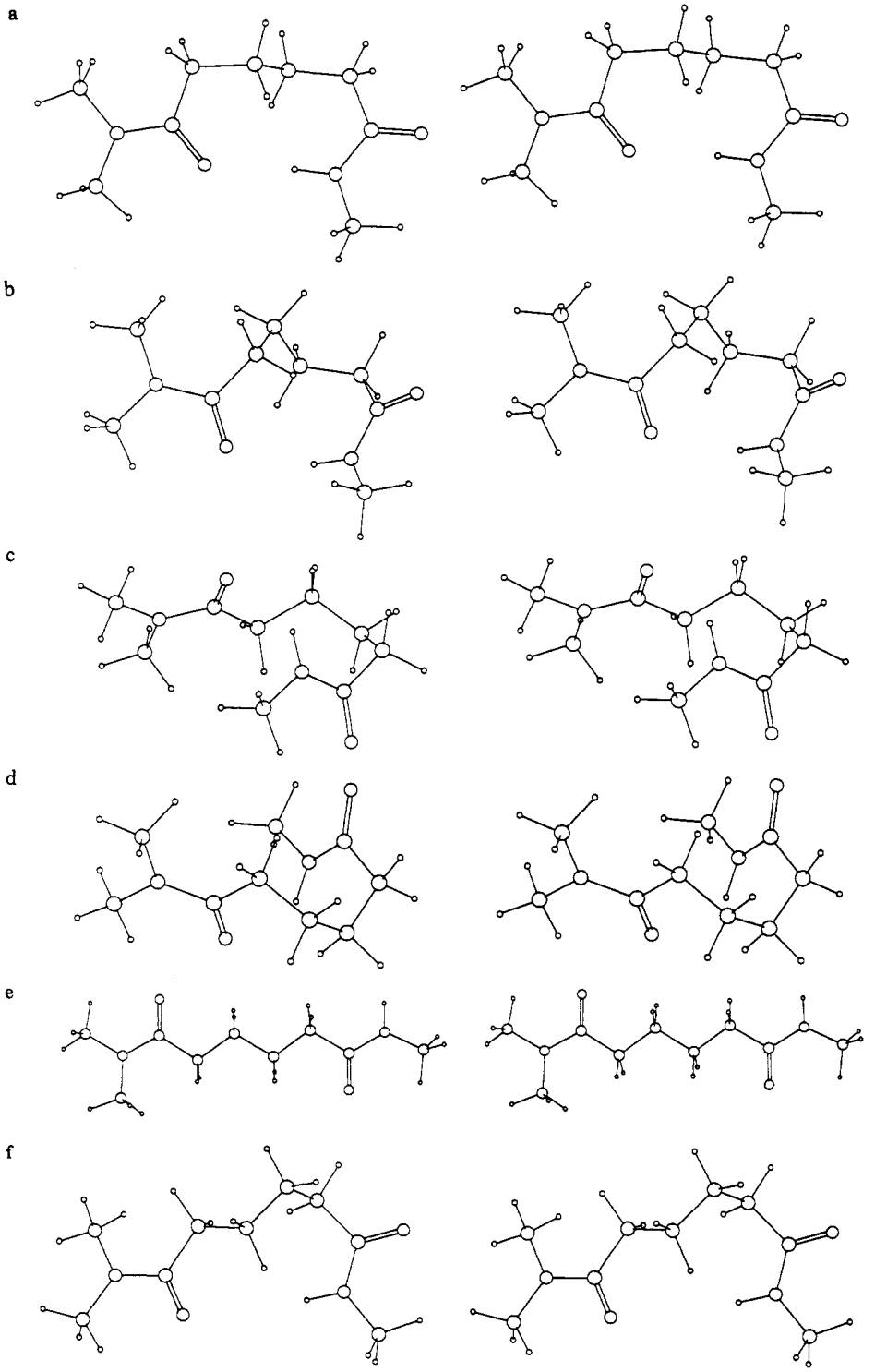

Figure 4. Stereoviews of several structures of diamide **2**(n=4): (a) **2a**(n=4), (b) **2b**(n=4), (c) **2c**(n=4), (d) **2d**(n=4), (e) **2e**(n=4), and (f) **2f**(n=4).

Table V. Heats of Formation (ΔH_f), Relative Energies ($\Delta\Delta E$), H···O Contact Distances ($r_{H\cdots O}$), N—H···O Contact Angle (∠N—H···O), and H···O═C Contact Angle (∠H···O═C) Calculated for Several Solvated Structures of Amides **2**(n = 1), **3**, and **1**

structure	H-bonded-ring size	$r_{H\cdots O}$, Å	∠N—H···O, deg	∠H···O═C, deg	ΔH_f, kcal/mol	$\Delta\Delta E$, kcal/mol
2a(n=1)·3(CH_2Cl_2)	6	2.604	120.6	82.1	−161.95	0.00
2c(n=1)·3(CH_2Cl_2)					−159.62	2.33
3a·3(CH_2Cl_2)	7	2.197	138.1	103.3	−172.16	0.00
3c·3(CH_2Cl_2)					−170.28	1.88
1b(d,u)·4(CH_2Cl_2)	6	2.431	120.3	87.7	−228.93	0.00
	7	2.184	141.4	100.6		
1e·4(CH_2Cl_2)	6	2.346	109.2	94.8	−228.79	0.14
	9	2.207	157.9	132.0		
1a·4(CH_2Cl_2)	6	2.314	125.1	90.2	−226.15	2.78
1d·4(CH_2Cl_2)					−225.99	2.80
	7	2.256	132.1	109.8		

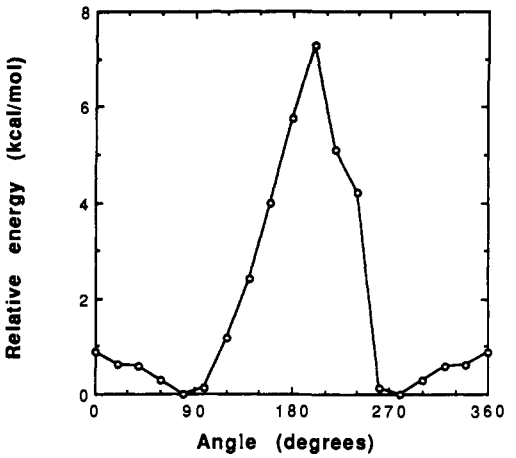

Figure 5. Potential curve of **2**(n=1) obtained as a function of the rotational angle θ (defined in **6**) from AM1 calculations.

as a function of ∠H···C=O, by performing SCF-MO calculations with the 6-31G** basis set. In these calculations, the H···O contact distance ($r_{H\cdots O}$) was optimized at each contact angle studied, and the formamide fragment geometries were kept frozen. The results of the above ab initio calculations were compared with those of the corresponding AM1 calculations in Figure 1a for ΔE vs ∠N—H···O and in Figure 1b for ΔE vs ∠H···O=C. In the 140–180° region of the ∠N—H···O or the ∠H···O=C variation, the interaction energy from the AM1 calculations is about 2 kcal/mol smaller in magnitude than that from the ab initio calculations. Both the AM1 and the ab initio calculations reveal that the interaction energy is nearly constant in the 140–180° region of the ∠N—H···O or ∠H···O=C angle variation.[13] This similarity suggests that AM1 and ab initio SCF-MO calculations provide a qualitatively similar description for the N—H···O=C hydrogen-bonding interaction, although they provide slightly different optimum contact angles. Therefore, AM1 calculations are expected to be adequate in describing the relative stabilities of the intramolecular hydrogen-bonding interactions of **1–3**.

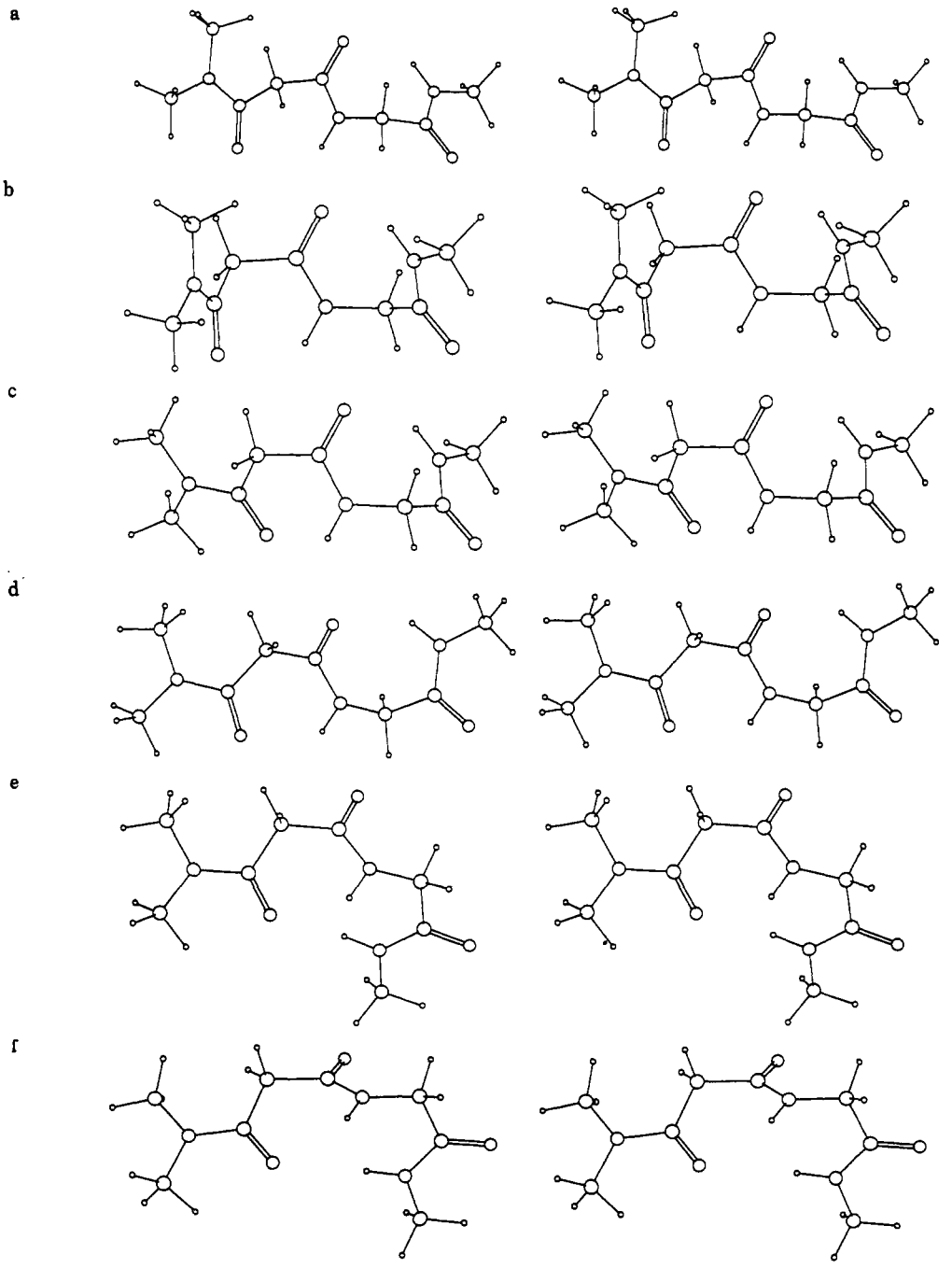

Figure 6. Stereoviews of several structures of triamide **1**: (a) **1d**(d,u), (b) **1b**(d,d), (c) **1b**(u,u), (d) **1b**(u,d), (e) **1e**, and (f) the transition state for the **1b**(u,u) → **1e** interconversion.

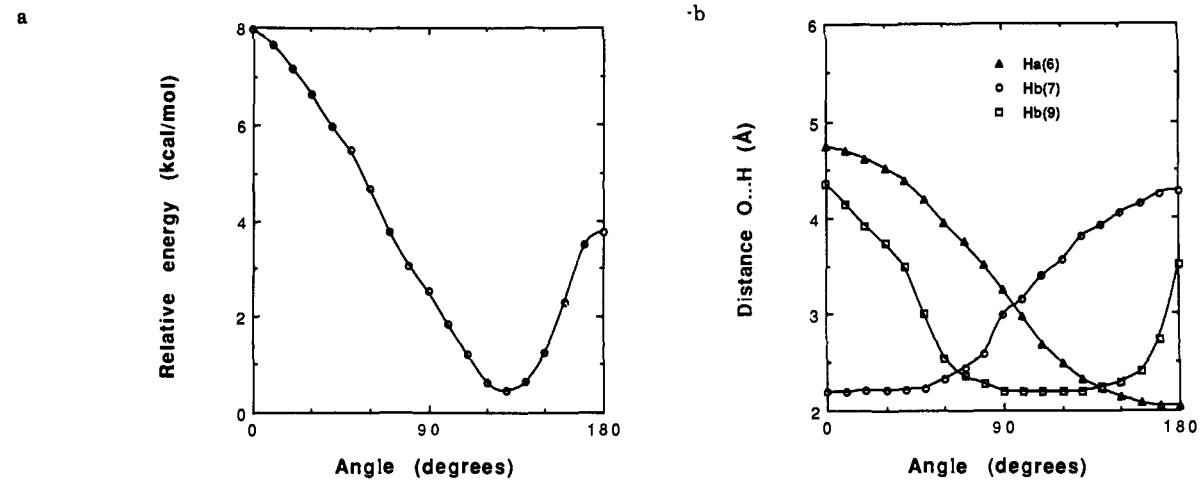

Figure 7. (a) Potential energy E_1 of triamide **1** as a function of θ_1 with **1e** as a starting conformation, where the energy is given with respect to that of **1b**(u,u). (b) Corresponding changes in the H···O contact distances as a function of θ_1.

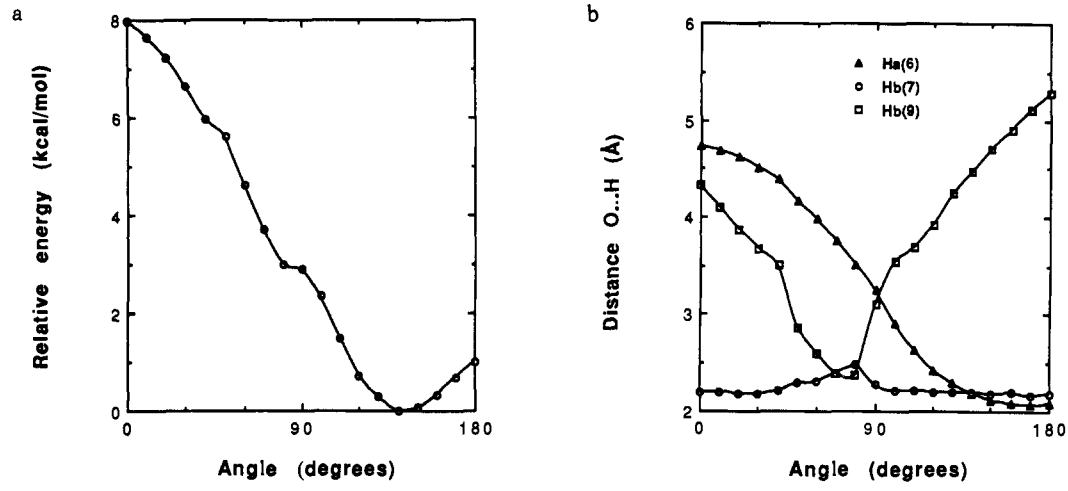

Figure 8. (a) Potential energy E_2 of triamide **1** as a function of θ_1 with **1b**(u,u) as a starting conformation, where the energy is given with respect to that of **1b**(u,u). (b) Corresponding changes in the H···O contact distances as a function of θ_1.

We now examine how the interaction energy of **5** depends upon $r_{H\cdots O}$, ∠N—H···O, and ∠H···O=C by performing AM1 calculations. Figure 2a shows a contour plot of the ΔE values obtained from AM1 calculations for **5** (for linear H···O=C and frozen fragment geometries) as a function of $r_{H\cdots O}$ and ∠N—H···O, Figure 2b that for **5** (with linear N—H···O and frozen fragment geometries) as a function of $r_{H\cdots O}$ and ∠H···O=C, and Figure 2c that for **5** as a function of ∠N—H···O and ∠H···O=C. It is clear from Figures 2a–c that the interaction energy surface is very soft with respect to the ∠N—H···O or the ∠H···O=C angle variation. This finding has an important implication concerning the intramolecular hydrogen-bonded conformations of **1–3**: Intramolecular N—H···O=C hydrogen bonding in these amides leads to a ring formation. The optimum structure of a hydrogen-bonded ring is determined primarily by a balance between the attractive interaction of the N—H···O=C hydrogen bonding and the associated ring strain. Since the energy surface of the hydrogen-bonding interaction is soft with respect to the ∠N—H···O and the ∠H···O=C angle variation, a rather wide range of these contact angles can be used to accommodate the ring geometries minimizing the strain.

Hydrogen-Bonded and Non-Hydrogen-Bonded Conformations of Amides 1–3

In a dilute solution of amides **1–3** in the very weakly hydrogen-bonding solvent CD_2Cl_2 or CH_2Cl_2, intermolecular hydrogen-bonding interactions between amide molecules are negligible.[3-5] However, an amide proton exchanges rapidly (on the NMR time scale) among its various intramolecular hydrogen-bonded and non-hydrogen-bonded conformations in equilibrium.[3-5] The temperature variation in the NMR studies of Gellman and coworkers covered the ~190–300 K region. Thus, for an equilibrium of amides **1–3**, stationary (i.e., minimum-energy) conformations with free energies which differ by more than 2 kcal/mol from the most stable one are unimportant. Therefore, we search for hydrogen-bonded and non-hydrogen-bonded conformations of **1–3** accessible for their equilibria.

A. Diamides 2 and 3. Table II lists the heats of formation (ΔH_f) and the relative energies ($\Delta\Delta E$) as well as the $r_{H\cdots O}$, ∠N—H···O, and ∠H···O=C values calculated for several conformations of diamides **2**(n=1–4) and **3**. Stereoviews of these hydrogen-bonded and non-hydrogen-bonded conformations for **2**(n=1) are shown in Figure 3, those for **2**(n=4) in Figure 4, and those for **2**(n=2,3) and **3** in supplementary Figures S1, S2, and S3. Important observations to note from these results are the following: (a) The most stable structures for **2**(n=1–4) and **3** are all hydrogen-bonded conformations. (b) For **2**(n=1) and **3**, non-hydrogen-bonded conformations are not stationary structures. (c) For **2**(n=2–4), the stability difference between the most stable hydrogen-bonded and the most stable non-hydrogen-bonded conformations decreases with increasing n. (d) For **2**(n=4), there exists a non-hydrogen-bonded conformation which is more stable than some hydrogen-bonded conformations. This is due most likely to the strain of the hydrogen-bonded rings.

Observation b is essentially related to the fact that the hydrogen-bonded ring of **2**(n=1) or **3** contains only one CH_2 group.

(13) Use of the STO-3G minimal basis set leads to a relatively stiff surface of interaction energy as a function of the ∠N—H···O angle. See: Peters, D.; Peters, J. *J. Mol. Struct.* **1980**, *68*, 255.

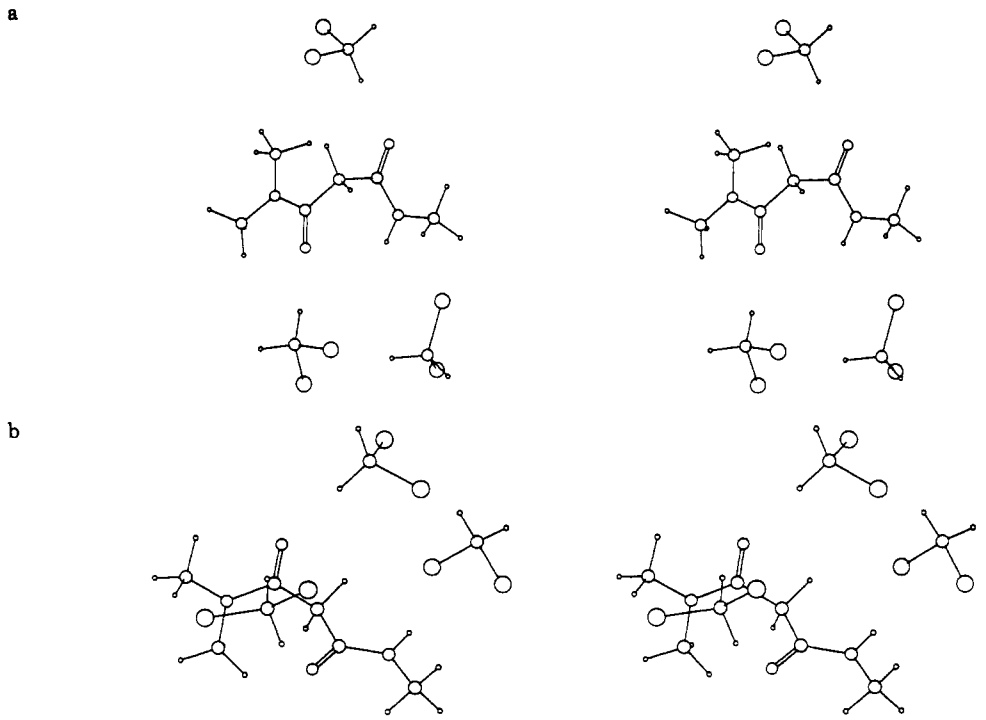

Figure 9. Stereoviews of two solvated structures of diamide **2**(n=1): (a) **2a**·3(CH_2Cl_2) and (b) **2c**·3(CH_2Cl_2).

The "open-chain" analogue of such a ring does not possess a single bond with a proper rotational barrier to keep the non-hydrogen-bonded form from collapsing into the hydrogen-bonded ring structure. In the 6- and 7-membered hydrogen-bonded rings of **2**(n=1) and **3**, the CH_2 group can tilt either "upward" or "downward" so that **2**(n=1) and **3** each have two minimum-energy conformations. Figure 5 shows the potential energy curve calculated for **2**(n=1) as a function of the rotational angle θ defined in **6**. The hydrogen-bonded conformation for θ = 0° is not a stationary structure and is converted to **2a**(n=1) or **2b**(n=1) when θ is allowed to relax.

Under the assumption that **2**(n=4) in CD_2Cl_2 or CH_2Cl_2 solution is in equilibrium between two states, i.e., hydrogen-bonded and non-hydrogen-bonded states, Gellman et al.[5] analyzed the temperature dependences of its IR and NMR spectra in terms of van't Hoff plots. According to this analysis, the hydrogen-bonded state is enthalpically more stable than the non-hydrogen-bonded state by about 1.5 kcal/mol. Here the hydrogen-bonded state represents a group of various hydrogen-bonded conformations [e.g., **2a–d**(n=4)], and the non-hydrogen-bonded state a group of various non-hydrogen-bonded conformations [e.g., **2e,f**(n=4)]. As in the case of **2**(n=4), the amide-proton chemical shift vs temperature (δ vs T) plot for a dilute CD_2Cl_2 solution of **2**(n=1) has a considerably negative slope.[4,5] Thus, for **2**(n=1) as well, the hydrogen-bonded state has a lower enthalpy than does the non-hydrogen-bonded state. For dilute CD_2Cl_2 solutions of diamides **2**(n=2,3) and **3**, however, the δ vs T plots are nearly flat although the slopes are still negative,[4,5] so that the hydrogen-bonded and non-hydrogen-bonded states are nearly equal in enthalpy. These findings are not necessarily incompatible with the present AM1 prediction of Table II that, for all diamides **2**(n=1–4) and **3**, the hydrogen-bonded conformations are generally more stable than the non-hydrogen-bonded conformations, because the solvation effects of CD_2Cl_2 molecules were neglected in the calculations. The hydrogen and oxygen atoms engaged in the N—H···O=C hydrogen bonding of an intramolecular hydrogen-bonded conformation are less available for the solvent molecules to make intermolecular hydrogen-bonding interactions with than are those in a non-hydrogen-bonded conformation. Thus, it is generally expected that the non-hydrogen-bonded state is stabilized more than is the hydrogen-bonded state by solvation with CD_2Cl_2 molecules. If the extent of this preferential stabilization is greater for diamides **2**(n=2,3) and **3** than for diamides **2**(n=1,4), then the relative stabilities of the hydrogen-bonded and non-hydrogen-bonded states of those diamides can be accounted for from our calculations.

B. Triamide 1. In each of the 6- and 7-membered hydrogen-bonded rings of **1b**, the CH_2 group can tilt "upward" or "downward" thereby generating four different stationary conformations **1b**(d,u), **1b**(d,d), **1b**(u,u), and **1b**(u,d) shown in Figure 6. Here we employ the terminology (d,u), (d,d), and so on to indicate whether the CH_2 groups of the 6- and 7-membered hydrogen-bonded rings are tilted "upward" or "downward". For instance, **1b**(d,u) means that the CH_2 group of the 6-membered ring is tilted downward but that of the 7-membered ring is tilted upward. These conformations are characterized by a short H_a···O contact forming a 6-membered hydrogen-bonded ring and a short H_b···O contact forming a 7-membered hydrogen-bonded ring [hereafter denoted by H_a···O(6) and H_b···O(7), respectively]. Conformation **1a** has a short H_a···O(6) contact, and conformation **1c** has a short H_b···O contact forming a 9-membered hydrogen-bonded ring [denoted by H_b···O(9)]. **1c** may also possess a short H_b···O(7) contact.[4] Other conformations relevant for triamide **1** are **1d** and **1e**. Conformation **1d** has a short H_b···O(7) contact, while conformation **1e** has short H_a···O(6) and H_b···O(9) contacts. Our AM1 calculations reveal that conformation **1e** is stationary, but conformations **1a**, **1c**, and **1d** are not. This finding is consistent with observation b discussed in the previous section. Namely, the H_a or H_b atom of conformations **1a**, **1c**, and **1d** can form a hydrogen-bonded ring containing one CH_2 group, so that they cannot be stationary structures. Table III lists the ΔH_f, $\Delta\Delta E$, $r_{H\cdots O}$, ∠N···H···O, and ∠H···O=C values calculated for **1e** and the four structures of **1b**.

Let us now examine how the intramolecular H_a···O(6), H_b···O(7), and H_b···O(9) contacts of **1b** and **1e** vary as a function of the dehedral angle θ_1 (between the planes containing the two carbonyl groups associated with the 6-membered hydrogen-bonded ring of **7**). For our study, conformation **1b**(u,u) is chosen as a representative example of **1b**. The potential energy of triamide **1**, as a function of θ_1, may be calculated with **1e** as a starting conformation (referred to as E_1 vs θ_1) or with **1b**(u,u) as a starting conformation (referred to as E_2 vs θ_1). Figures 7a and 8a show the E_1 vs θ_1 and E_2 vs θ_1 plots for θ_1 = 0–180°, respectively. Figures 7b and 8b plot the changes in the H···O contact distances

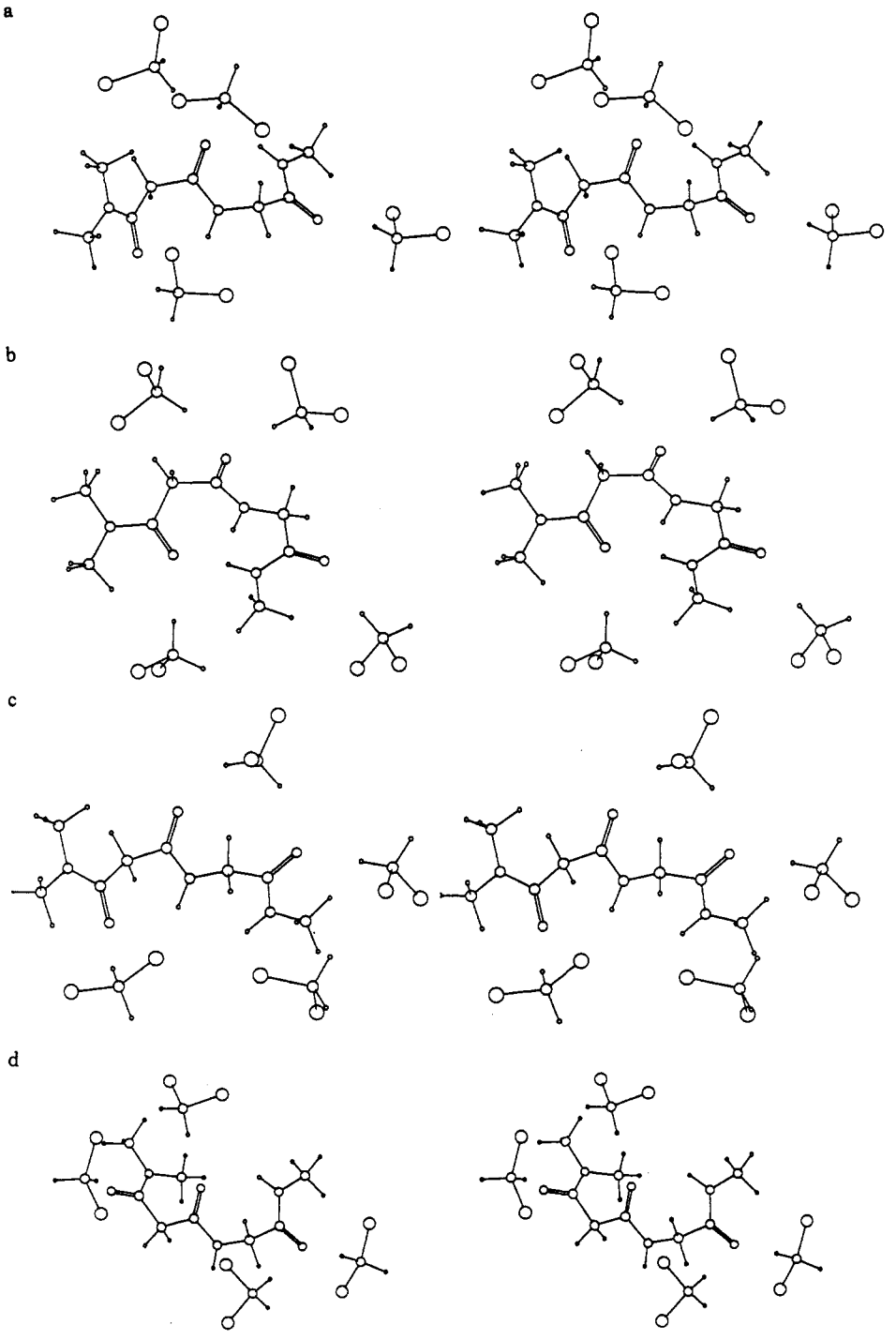

Figure 10. Stereoviews of four solvated structures of triamide **1**: (a) **1b**(d,u)·4(CH_2Cl_2), (b) **1e**·4(CH_2Cl_2), (c) **1a**·4(CH_2Cl_2), and (d) **1d**·4(CH_2Cl_2).

corresponding to the potential curves of Figures 7a and 8a, respectively. In the region of θ_1 = 0–80°, the conformations associated with the E_1 vs θ_1 curve are very similar to those associated with the E_2 vs θ_1 curve. Conformation **1d** is characterized by $\theta_1 \cong 0°$, and **1c** by $\theta_1 \cong$ 60–80°. In the region of $\theta_1 \cong$ 80–180°, the conformations associated with the E_1 vs θ_1 curve differ considerably from those for the E_2 vs θ_1 curve. Figures 7 and 8 clearly show that conformations **1b**(u,u) and **1e** are stationary, but conformations **1a**, **1c**, and **1d** are not. That **1c** is not a stationary structure is consistent with our finding that the only stationary structure of **2**(n=1) is a hydrogen-bonded conformation. There are three main factors responsible for making **1c** a non-stationary structure: the N—H_a···O=C hydrogen-bond formation, which leads to a six-membered hydrogen-bonded ring, the removal of the oxygen-oxygen repulsion between the two carbonyl groups in the resulting six-membered ring, and the presence of a rotational path leading **1c** to **1e**. Conformations **1b**(u,u) and **1e** can be interconverted by varying the dihedral angle θ_2 (between the planes containing the two carbonyl groups associated with the 7-membered hydrogen-bonded ring of **7**). Our AM1 calculations show that the transition state for the **1b**(u,u) → **1e** interconversion is less stable than **1b**(u,u) by 2.64 kcal/mol, and that the H_a···O(6), H_b···O(7), and H_b···O(9) contact distances of the transition state are 2.180, 3.067, and 2.882 Å, respectively. A stereoview of this transition state is shown in Figure 6e.

Our finding that **1a** and **1c** are not stationary conformations should be examined further because the stabilities of the amide conformations calculated in our work refer to those expected in the absence of solvent molecules. The IR spectra of **2**(n=1) and **3** in dilute CH_2Cl_2 solution reveal the presence of non-hydrogen-bonded states,[4,5] so that stationary non-hydrogen-bonded conformations must be present in the solutions. Our AM1 cal-

culations neglecting solvation effects show that non-hydrogen-bonded structures of **2**(n=1) and **3** are not stationary conformations. Therefore, it is necessary to investigate how the stabilities of amide conformations are modified by solvation with CH_2Cl_2 molecules.

Solvation Effect

Simulation studies[14] are needed to properly describe the energetics of various amide conformations in dilute CD_2Cl_2 or CH_2Cl_2 solution. However, the qualitative aspects of the solvation effect on the structure of a solute molecule can be reasonably well described in terms of a supermolecule consisting of a solute and several solvent molecules.[15] In the present work, we focus upon the question of whether or not the conformations **2c**(n=1), **3c**, **1a**, **1c**, and **1d** become stationary structures when solvated with several CH_2Cl_2 molecules. Thus we carry out AM1 calculations on the appropriate amide·$m(CH_2Cl_2)$ (m = integer) complexes. For such calculations, one needs to know preferred arrangements and strengths of interactions between amide and CH_2Cl_2 molecules and also between CH_2Cl_2 molecules. For this purpose, we perform AM1 calculations on the three arrangements **8a**–**c** of H_2N—C—H=O···CH_2Cl_2 and the two arrangements **9a**,**b** of CH_2Cl_2···C—H_2Cl_2. The strengths of the C—H···O=C and N—H···Cl—C contact interactions between H_2N—CH=O and CH_2Cl_2 were estimated on the basis of the linear arrangements **8a** and **8b**, respectively, to avoid a collapse into the more stable structure **8c**. Table IV summarizes the optimum contact distances and the interaction energies calculated for **8a**–**c** and **9a**,**b**. The C—H···O=C interaction energy between CH_2Cl_2 and H_2N—CH=O is quite large, but it may be an artifact of AM1 calculations. What is important for our study is the finding that the C—H···O=C contact interaction is substantially more attractive than the N—H···Cl—C or the C—H···Cl—C contact interaction. Thus, an optimum arrangement of an amide·$m(CH_2Cl_2)$ complex is obtained by capping each carbonyl oxygen atom with at least one CH_2Cl_2 molecule via an intermolecular C—H···O=C contact.

In the following we examine how the relative stabilities of intramolecular hydrogen-bonded and non-hydrogen-bonded amide conformations are affected when these conformations make intermolecular contacts with solvent molecules by fully optimizing the appropriate amide·$m(CH_2Cl_2)$ supermolecules. In the AM1 calculations of amide·$m(CH_2Cl_2)$, we employ a limited number of solvent molecules (i.e., m = 3 for diamides **2**(n=1) and **3**, and m = 4 for triamide **1**). Therefore, in order to have a meaningful comparison for the relative energies of different amide conformations in CH_2Cl_2 solution, it is necessary to make sure that these conformations possess similar intermolecular contacts with solvent molecules.

We examine how solvation affects the relative stabilities of **2a**(n=1), **2c**(n=1), **3a**, and **3c** by performing AM1 calculations on the corresponding amides solvated with three CH_2Cl_2 molecules. The optimized structures of **2a**(n=1)·3(CH_2Cl_2) and **2c**(n=1)·3-(CH_2Cl_2) are shown as stereoviews in Figure 9, and those of **3a**·3(CH_2Cl_2) and **3c**·3(CH_2Cl_2) in supplementary Figure S4. The ΔH_f, $\Delta\Delta E$, $r_{H\cdots O}$, ∠N—H···O, and ∠H···O=C values obtained for these structures are listed in Table V. The solvated non-hydrogen-bonded conformations **2c**(n=1)·3(CH_2Cl_2) and **3c**·3-(CH_2Cl_2) are stationary structures, which is consistent with the observation that dilute solutions of **2**(n=1) and **3** exhibit non-hydrogen-bonded states.[4,5] As expected, the non-hydrogen-bonded conformations of **2**(n=1) and **3** are less stable than their respective hydrogen-bonded conformations even under solvation.

We performed AM1 calculations of the IR spectra expected for the supermolecules **2a**(n=1)·3(CH_2Cl_2) and **2c**(n=1)·3-(CH_2Cl_2). The absorption maximum of the calculated N-H stretching occurs at 3450 cm^{-1} for the hydrogen-bonded structure **2a**(n=1)·3(CH_2Cl_2), and at 3510 cm^{-1} for the non-hydrogen-bonded structure **2c**(n=1)·3(CH_2Cl_2). The calculated red shift of 60 cm^{-1}, associated with the intramolecular N—H···O=C hydrogen bonding in **2**(n=1), is in reasonable agreement with the experimental value of 140 cm^{-1} (i.e, 3310 vs 3450 cm^{-1}).[4]

Table V also summarizes results of our AM1 calculations on triamide **1** solvated with four CH_2Cl_2 molecules. The optimized structures of **1a**·4(CH_2Cl_2), **1b**(d,u)·4(CH_2Cl_2), **1d**·4(CH_2Cl_2), and **1e**·4(CH_2Cl_2) are shown as stereoviews in Figure 10. The solvated structures **1a**·4(CH_2Cl_2) and **1d**·4(CH_2Cl_2) are stationary structures, and are less stable than the solvated structures **1b**-(d,u)·4(CH_2Cl_2) and **1e**·4(CH_2Cl_2). This is not surprising because only one amide hydrogen atom participates in hydrogen bonding in the former but both amide hydrogen atoms do in the latter. We attempted to make conformation **1c** a stationary structure by solvating with four CH_2Cl_2 molecules, but full geometry optimizations of **1c**·4(CH_2Cl_2) lead to either **1b**·4(CH_2Cl_2) or **1e**·4(CH_2Cl_2) as in the case of unsolvated **1c**. As a function of the dihedral angle θ_1 in the vicinity of **1e**·4(CH_2Cl_2), the potential energy curve is calculated to be slightly softer than the corresponding curve obtained for unsolvated **1e** (i.e., the E_2 vs θ_1 plot in Figure 8a). That the crystal structure[6] of **1** adopts conformation **1c** is a consequence of attractive intermolecular interactions involving the H_a atom (i.e., intermolecular N—H···O=C hydrogen-bonding interactions).

Concluding Remarks

According to the present ab initio and AM1 calculations, the energy surface of the N—H···O=C hydrogen-bonding interaction is soft with respect to the ∠N—H···O and ∠H···O=C angle variations. Consequently, for intramolecular hydrogen-bonded conformations of amides, a rather wide range of these contact angles can be used to accommodate their ring structures minimizing the associated strain. Our AM1 calculations show that the most stable structure of a given amide is a hydrogen-bonded conformation, and that the stability of triamide **1** increases with an increase in the number of intramolecular N—H···O=C hydrogen-bonding contacts. It is noteworthy that conformation **1b** with 6- and 7-membered hydrogen-bonded rings is similar in stability to conformation **1e** with 6- and 9-membered hydrogen-bonded rings. The amide conformations **2c**(n=1), **3c**, **1a**, and **1d** become stationary structures only when solvated with CH_2Cl_2 molecules. However, **1c** is not a stationary structure even when solvated with four molecules, and is not likely to become one even if solvated with a larger number of CH_2Cl_2 molecules. Furthermore, conformation **1e**, which was not considered in Gellman et al.'s study,[4] is a stationary structure nearly as stable as **1b**. The stationary conformations that triamide **1** can adopt in dilute CH_2Cl_2 solution are **1a**, **1b**, **1d**, and **1e**. In view of this finding, it seems necessary to re-interpret the temperature-dependent NMR data[4] of **1** in terms of an equilibrium involving only these stationary structures.

Acknowledgment. This work was supported by the U.S. Department of Energy, Office of Basic Energy Sciences, Division of Materials Science, under Grant DE-FG05-86ER45259. J.J.N. thanks NATO and Ministerio de Educacion y Ciencia (Spain) for Fellowships, which made it possible to visit North Carolina State University, and DGICYT PB89-0268. We thank Professor S. H. Gellman for invaluable comments and discussion.

Registry No. 1, 131042-62-1; **1**·4(CH_2Cl_2), 136706-25-7; **2** (n = 1), 125111-72-0; **2** (n = 2), 27846-70-4; **2** (n = 3), 125111-73-1; **2** (n = 4), 1862-10-8; **2** (n = 1)·3(CH_2Cl_2), 136706-26-8; **3**, 136228-20-1; **3**·3-(CH_2Cl_2), 136706-27-9; **4**, 75-12-7; dichloromethane, 75-09-2.

Supplementary Material Available: Stereoviews of several structures of diamide **2**(n = 2, 3), diamide **3**, and solvated diamide **3**·3(CH_2Cl_2) (4 pages). Ordering information is given on any current masthead page.

(14) (a) Owicki, J. C.; Scheraga, H. A. *J. Am. Chem. Soc.* **1977**, *99*, 7403. (b) Rossky, D. J.; Karplus, M. *J. Am. Chem. Soc.* **1979**, *101*, 1913. (c) Romano, S.; Clementi, E. *Int. J. Quantum Chem.* **1980**, *17*, 1007. (d) Mezei, M.; Beveridge, D. *J. Chem. Phys.* **1981**, *74*, 6902. (e) Jorgensen, W. L. *J. Phys. Chem.* **1983**, *87*, 5304. (f) Jorgensen, W. L. *Acc. Chem. Res.* **1989**, *22*, 184. (g) Dang, L. X.; Rice, J. E.; Caldwell, J.; Kollman, P. A. *J. Am. Chem. Soc.* **1991**, *113*, 2481. (h) Hagler, A. T.; Osguthorpe, D. J.; Robson, B. *Science* **1980**, *208*, 599.

(15) Tapia, O. *Molecular Interactions*; Ratajczak, H., Orville-Thomas, W. R., Eds.: Wiley: New York, 1982; Vol. 3, p 47.